Molecular Crystals and Liquid Crystals Science and Technology. Section A. Molecular Crystals and Liquid Crystals

Publication details, including instructions for authors and subscription information:
http://www.tandfonline.com/loi/gmcl19

Spin Densities in Bimetallic Compounds: Polarized Neutron Diffraction

Béatrice Gillon [a]

[a] Laboratoire Léon Brillouin (C.E.A.-C.N.R.S.), C.E.N. Saclay, 91191, Gif-sur-Yvette, FRANCE

Version of record first published: 24 Sep 2006

To cite this article: Béatrice Gillon (1999): Spin Densities in Bimetallic Compounds: Polarized Neutron Diffraction, Molecular Crystals and Liquid Crystals Science and Technology. Section A. Molecular Crystals and Liquid Crystals, 335:1, 53-72

To link to this article: http://dx.doi.org/10.1080/10587259908028851

Mol. Cryst. and Liq. Cryst., 1999, Vol. 335, pp. 53-72
Reprints available directly from the publisher
Photocopying permitted by license only

Spin Densities in Bimetallic Compounds: Polarized Neutron Diffraction

BÉATRICE GILLON

Laboratoire Léon Brillouin (C.E.A.- C.N.R.S.), C.E.N. Saclay, 91191 Gif-sur-Yvette, FRANCE

The determination of the spin density map in molecular magnetic compounds provides crucial informations about the phenomena playing a role in magnetic interactions, like spin delocalization and spin polarization. Polarized neutron diffraction on single crystals is the unique experimental technique which allows to visualize the spin distribution over a whole molecule. A review of spin density studies in bimetallic compounds will be presented as well as very recent results obtained on the induced spin density distribution along a ferromagnetic Mn(II)Ni(II) bimetallic chain.

Keywords: spin density; neutron diffraction; polarized neutrons; bimetallic compounds

INTRODUCTION

Polarized neutron diffraction (p.n.d.) is a well established technique for spin density determinations in single crystals[1]. This experimental method has been successfully applied in the eighties to magnetic molecular compounds such as organic radicals[2], transition metal complexes[3] or bimetallic compounds[4, 5]. While X-ray diffraction permits to determine the total electronic density in a

crystal, p.n.d. gives access to the spin density due to the unpaired electrons of the outer valence shells. In transition metal complexes, the formation of metal-ligand bonds leads to a redistribution of the spin in the molecular orbitals built on the 3d transition ion orbitals and the s and p ligand orbitals, and therefore to the delocalization of the spin over the molecule.

In an Unrestricted-Hartree-Fock description of the molecular wave function, the spin density $\rho(\vec{r})$ is written as the difference between the density of electrons with α spin and the density of electrons with β spin: $\rho(\vec{r}) = \rho_\alpha - \rho_\beta$. This expression shows that the spin density may be negative in some regions of space. An obvious reason for that is antiferromagnetic (AF) intramolecular coupling between two magnetic centers such as in heterobimetallic compounds. Because the spins are aligned by an external field, the atoms carrying the majority spin correspond to positive regions and those which are AF coupled to the former ones carry a negative spin density. The second possible origin of negative spin density is spin polarization[6]. While spin delocalization from a spin carrier towards its first nearest neighbours leads to the apparition of a spin density of the same sign, the spin polarization effect on the next nearest neighbours induces a spin density of the opposite sign.

The role of the spin delocalization on the organic bridge in AF coupled heterobimetallic systems will be discussed at the light of the p.n.d. investigations of a 'short bridge' compound Cu(II)Ni(II)[5] and 'extended bridge' Mn(II)Cu(II) compounds: a molecular oxamido-bridged compound[7] and an oxamato-bridged ferrimagnetic chain compound[8].

The origin of the strong intramolecular ferromagnetic coupling in di-μ-1,1-azido Cu^{2+} dinuclear compounds has been the subject of a long controversy[9]. The determination of the induced spin density in the $[Cu_2(t\text{-}Bupy)_4(N_3)_2](ClO_4)_2$ compound in the triplet ground state[10] allows a discussion of the two main proposed mechanisms: the spin polarization mechanism[11] and accidental orthogonality like in the di-hydroxo-dicopper compound[4].

The recent results obtained on the ferromagnetic chain compound $MnNi(NO_2)_4(en)_2$ (with en = ethylenediamine)[12] are reported in this paper.

The induced spin distribution along the zig-zag chain constituted by alternating Ni^{2+} and Mn^{2+} ions bridged by a bidendate NO_2^- group is presented and discussed in term of spin delocalization and spin polarization effects.

SPIN DENSITY DETERMINATION: POLARIZED NEUTRON DIFFRACTION

The aim of p.n.d. is to determine the magnetic structure factors, which are the Fourier components of the magnetization density:

$$F_M(\vec{K}) = \int_{cell} \rho(\vec{r}) e^{i\vec{K}\vec{r}} \, d\vec{r} \qquad (2)$$

The magnetization density is then reconstructed[13] either by direct methods like the Fourier summation or Maximum of Entropy methods, or by modelling the spin density.

Principles

Two main phenomena contribute to the diffracted intensity of a neutron beam by a magnetically ordered single crystal: nuclear scattering and magnetic scattering due to the dipolar magnetic interaction between the neutron magnetic moment and the unpaired electron magnetic moments in the crystal. In the case of paramagnetic species, the unpaired electron magnetic moments are aligned by an external magnetic field.

The p.n.d. technique consists in measuring the ratio R between the diffracted intensities I_+ and I_- on the Bragg peaks without and with reversal of the neutron polarization of the incident beam. The neutron polarization is vertical and parallel to the applied magnetic field. These intensities I_+ (or I_-) are respectively equal to the square of the sum (or of the difference) of the nuclear and magnetic structure factors F_N and F_M. The so-called flipping ratio R is usually written in term of γ which is the ratio between the magnetic and nuclear structure factors:

$$R(\vec{K}) = \frac{(1+\gamma)^2}{(1-\gamma)^2} \qquad (3)$$

where $\vec{K}$ is the scattering vector. This expression is valid for reflections in the horizontal plane in the ideal case where the polarization of the incident beam and the flipping efficiency are equal to one.

The nuclear structure factors are defined by:

$$F_N(\vec{K}) = \Sigma_i\, b_i\, e^{i\vec{K}\vec{r}_i}\, e^{-W_i} \qquad (4)$$

where i refers to the atoms contained in the elementar cell, b_i is the nuclear scattering length characteristical for each chemical element and W_i is a thermal factor.

For centrosymmetric crystals, both magnetic and nuclear structure factors are real and from Equ.(3) it is possible to deduce F_M knowing F_N. Therefore the precision obtained on F_M depends also on the quality of the structure determination, which has to be performed with help of unpolarized neutron diffraction in order to localize the hydrogen atoms, the position of which is not provided by X-ray diffraction.

The magnetization density is the sum of a pure-spin contribution and of an orbital contribution due to the interaction between the neutron magnetic moment and the magnetic field created by the unpaired electrons moving on their orbits. However for most of the transition metals of the first row the orbital moment is almost entirely quenched[14] and the orbital contribution can be neglected or treated as a correction[15]. The magnetization density is identical to the spin density in the case of systems with zero angular momentum, like for 3d transition metal ions with half filled 3d shell.

Data analysis

The p.n.d. data consist of a set of N experimental magnetic structure factors $F_M^{obs}(\vec{K})$ from which the spin density can directly be reconstructed either by Fourier summation or by the Maximum of Entropy method. The Fourier summation method is often unsatisfactory because of the limited number of

observations which leads to severe truncation effects. A new method, based on the Maximum of Entropy, has emerged a few years ago[16]: it selects the most probable spin density map which is compatible with the data. This map $\rho(\vec{r})$ is obtained by maximizing the entropy under the condition $\chi^2 = N$ in order to keep a good value of the agreement factor $\chi^2 = \sum_K^N | (|F_M^{obs}| - |F_M^{cal}|) / \sigma |^2$ where F_M^{obs} is the observed magnetic structure factor with error bar σ and F_M^{cal} is calculated from the map $\rho(\vec{r})$.

Beyond the direct spin density reconstruction, an other way to analyze the p.n.d. data consists in refining a model of the spin density by a least-squares procedure[17]. The spin density $\rho(\vec{r})$ is assumed to be the sum of atomic densities $\rho_i(\vec{r_i})$ centered on the atoms i. The multipole model initially proposed for charge density studies has been adapted for spin density[2]. Each atomic density is developped over a basis of multipole functions which are product of a radial function $R_l^i(r)$ and a real spherical harmonics $y_{lm}^i(\theta,\phi)$:

$$\rho_i(\vec{r_i}) = \sum_{l=0}^{4} \sum_{m=-l}^{l} P_{lm}^i R_l^i(r_i) y_{lm}^i(\theta_i,\phi_i) \qquad (5)$$

The radial function is a Slater-type function $R_l^i(r_i) = N_l r_i^{n_l} e^{-\zeta_i r_i}$. The parameters to be refined are the multipole populations P_{lm}^i and the radial exponents ζ_i.

In order to analyze the spin density in term of atomic orbital populations, an exact analogy has been established between the multipole description (5) and the expression of $\rho_i(\vec{r_i})$ deduced from the wave function. In a restricted Hartree-Fock scheme, the spin density centered on an atom with only one unpaired electron is expressed as:

$$\rho_i(\vec{r_i}) = |\psi_i(\vec{r_i})|^2 \qquad (6)$$

where $\psi_i(\vec{r_i})$ is the wave function of the unpaired electron:

$$\psi_i(\vec{r_i}) = \sum_{m'=-l'}^{l'} a_{l'm'}^i R_{l'}^i(r_i) y_{l'm'}^i(\theta_i,\phi_i) \qquad (7)$$

where $l' = 0, 1, 2$ for s, p, d orbitals and with the normalization condition $\sum_{m'=-l'}^{l'} a_{l'm'}^{i\,2} = 1$. The expression (6) has to be multiplied by an atomic population coefficient P_i which can be negative. The development of

expression (6) using (7) provides direct relationships between the multipole parameters P^i_{lm} and the wave function parameters, P_i and $a^i_{l'm'}$, taking into account that the product of two Slater-type functions is a Slater-type function with $n = (n'+n'')$ and $\zeta = (\xi'+\xi'')$ and that the product of two real spherical harmonics is a linear combination of real spherical harmonics[18]. These relationships are used either to refine the orbital coefficients or to apply 2p or 3d-type constraints on the atomic spin densities.

SPIN DELOCALIZATION IN ANTIFERROMAGNETICALLY COUPLED BIMETALLIC COMPOUNDS

An illustrative example of spin delocalization in an AF coupled bimetallic compound is provided by the spin density study in the compound $Cu(salen)Ni(hfa)_2$ with salen = N,N'-ethylenebis(oxosalicyldiiminato) and hfa = hexafluoroacetylacetonato. The non-planarity of the CuO_2Ni bridging network in this compound leads to a rather short Cu .. Ni distance of 2.91 Å. In Fig. 1. is represented the spin density induced in the doublet ground state[5]. Constraints on the Cu^{2+} and Ni^{2+} local symmetry were applied to the multipole model and 2p-type densities were assumed for the oxygen atoms except for the bridge. The AF interaction between Cu(II) and Ni(II) is reflected by the observation of two spin density regions of opposite signs corresponding respectively to the copper and nickel ions surrounded by their first neighbours, which carry respectively a total moment of $-0.22(1)\mu_B$ and $1.11(1)\mu_B$.

While a spin delocalization towards the atoms external to the bridge can be observed, no spin resides on the bridge within the experimental uncertainty ($0.01\mu_B$). A negative spin transfer from Cu(II) towards the neighbouring nitrogen atoms occurs together with a positive spin transfer from Ni(II) towards the terminal oxygen atoms which carry about $0.04(1)\mu_B$ each. The experimental spin distribution is remarkably well reproduced in the electron active model using natural magnetic orbitals[6] . The zero spin density on the phenolic atoms results from the exact compensation between the positive spin

density transferred from Ni(II) and the negative spin transferred from Cu(II), although the moment on Cu^{2+} is much smaller than on Ni^{2+}. The absence of any spin density on the phenolic atoms demonstrates that the magnetic orbitals centered on Cu(II) and Ni(II) actually overlap on these atoms, which leads to an AF intramolecular interaction.

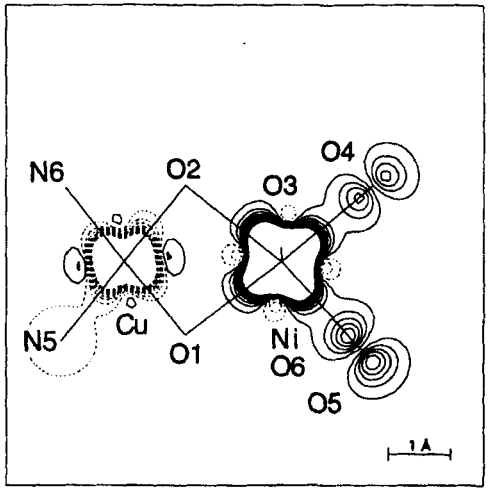

FIGURE 1 Induced spin density map for Cu(salen)Ni(hfa)$_2$ at 2K under 5 Teslas integrated along the Ni-O6 direction. The solid lines represent positive levels and dashed lines are negative levels. Only the low-level lines are plotted: 0.005 $\mu_B/Å^2$ by step of $\pm$ 0.010 $\mu_B/Å^2$.

The AF coupling through the extended oxamido bridge in the molecular compound [Mn(cth)Cu(oxpn)](CF$_3$SO$_3$)$_2$ where cth = (Me$_6$-[14]ane-N$_4$) and oxpn = N,N'-bis(3-aminopropyl)oxamido (J = -31.1cm^{-1}) is stronger than the coupling in the Cu(II)Ni(II) compound (J = -23.6 cm^{-1}), although the distance between the metallic ions is much larger ($d_{Mn...Cu}$ = 5.44Å)[19]. The ability of the oxamido bridge to propagate an AF interaction between the two transition metal ions is directly connected to its unsaturated character and to the quasi-

coplanarity between the Mn^{2+} and Cu^{2+} basal planes and the oxamido plane. The induced spin density map in Fig. 2. visualizes the spin delocalization over the whole molecule $[Mn(cth)Cu(oxpn)]^{2+}$ in the quintet ground state[7]. A spherical model was applied to the Mn^{2+} spin distribution assuming equal occupations of the five 3d orbitals[7]. The Cu^{2+} spin density was constrained to be of $3d_{x^2-y^2}$ type. Due to the low values of the spin populations on the nitrogen, oxygen and carbon atoms, spherical spin densities only were refined on these atoms. Like for the Cu(II)Ni(II) compound, the opposite signs of the spin densities associated to the magnetic centers and their surroundings reflect the negative intramolecular coupling.

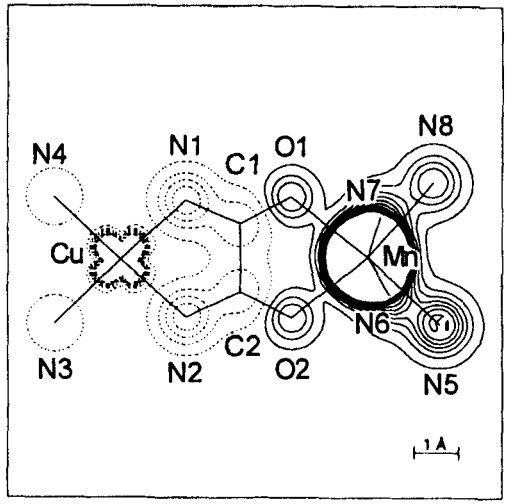

FIGURE 2 Induced spin density map for $[Mn(cth)Cu(oxpn)](CF_3SO_3)_2$ at 2K under 5 Teslas in projection along the perpendicular to the oxamido mean plane. Same levels as in Fig. 1.

The sum of the positive spin populations is equal to $4.67(8)\mu_B$ and the sum of the negative populations amounts $-0.67(8)\mu_B$. The Cu^{2+} spin population represents only 70 per cent of the total negative population while the Mn^{2+} ion

carries 93 per cent of the total positive population. This reflects the more pronounced covalent character of Cu(II) - ligand bonds compared to Mn(II) - ligand bonds.

Local Spin Density ab initio calculations on the precursor Cu[oxpn][20] demonstrate that the spin transfer from Cu(II) towards the oxamido group leads to significant contributions both on the nitrogen atoms and on the terminal oxygen atoms. L.S.D. calculations on an idealized fragment centered on Mn(II)[7] show in a similar way, but to a smaller extent, a delocalized moment on the oxygen atoms and a small contribution on the terminal nitrogen atoms of the oxamido group. Because of the strong delocalization from copper over the whole bridge, the magnetic orbitals centered on Cu(II) and Mn(II) respectively strongly overlap on the oxygen atoms of the oxamido bridge, giving rise to an antiferromagnetic coupling between copper and manganese.

It should be noticed that the L.S.D. calculations of the copper precursor and of the Mn(II)-centered fragment give evidence for a spin polarization of the π orbitals of the carbon atoms of the oxamido group. The small observed negative spin density on these carbon atoms can then be interpreted as resulting from a dominant spin polarization effect originating from manganese.

Very similar features have been observed for the spin delocalization on the oxamato bridge in the ferrimagnetic chain compound $MnCu(pba)(H_2O)_3.2H_2O$[8] with pba = 1,3-propylenebis(oxamato). The oxamato bridge differs from the oxamido bridge by one oxygen atom replacing one nitrogen atom. The smaller value of the coupling constant ($J = -23.4\ cm^{-1}$) is directly related to the weaker spin delocalization on the oxamato bridge which is due, on one hand, to the smaller spin transfer from Cu(II) towards oxygen ($-0.05(1)\mu_B$) than towards nitrogen ($-0.08(1)\mu_B$) and, on the other hand, to the deviation from planarity of the Mn(oxamato)Cu bridging network in the chain compound.

SPIN POLARIZATION OF THE AZIDO BRIDGES IN A di-μ-1,1-AZIDO Cu(II) BINUCLEAR COMPOUND

The remarkable ability of the azido bridge N_3^- to induce a strong ferromagnetic interaction in di-μ-azido Cu(II) bimetallic compounds, when it bridges in the 1,1-fashion, has been interpreted by a mechanism involving a spin polarization of the π_g highest occupied molecular orbital of the azido bridge N_3^- [11]. This mechanism implies that the bridging nitrogen atom of the azido group carries a negative spin. All the di-μ-1,1-azido Cu^{2+} binuclear compounds are then expected to present a triplet ground state, which has been observed until now for all the synthetized compounds of this type.

The other possible interpretation is the accidental orthogonality of the magnetic orbitals[6] similarly to the case of planar di-μ-hydroxo-bridged copper(II) dimers. It has been established for these compounds than the intramolecular interaction is ferromagnetic for a Cu-O-Cu dihedral angle smaller than 97.5°, that is close to 90°. Owing to the systematic study of dicopper compounds with asymmetrical bridges consisting of a μ-1,1-azido bridge and a μ-1,2-diazine bridge [9], a value of 108° has been proposed for the Cu-N-Cu dihedral angle at which the cross-over between the ferro- and AF couplings would occur in di-μ-1,1-azido Cu^{2+} binuclear compounds. On the contrary to the first mechanism, a positive spin density is expected on the bridging nitrogen atom, due to the spin delocalization from each Cu^{2+} ion.

The induced spin density map in the triplet ground state of Cu_2(t-Bupy)$_4$(N$_3$)$_2$ (ClO$_4$)$_2$[10] shown in Fig. 3. gives evidence for the delocalization of positive spin density from the copper ions which carry 0.738(7)μ_B each towards the terminal N3 and bridging N1 nitrogen atoms of the azido group as well as towards the t-Bupy nitrogen atoms N4 and N5. A $3d_{x^2-y^2}$ constraint was applied to the Cu^{2+} ion. Different constraints ($2p_\sigma$ or $2p_\pi$ type) were checked for the nitrogen atoms[10]. On the terminal N3 atom of the azido bridge only, a $2p_z$-type constraint was found to improve slightly the spherical model. The N1 and N3 nitrogen atoms of the azido bridge carry about the same spin amount: 0.069(6)μ_B on N1 and 0.057(7)μ_B on N3, while a small negative

spin population of -0.016(6)μ_B is observed on the central nitrogen N2. The spin transfer on the nitrogen atoms of the t-Bupy ligands N4 (0.067(8)μ_B) and N5 (0.049(7)μ_B) is of the same order of magnitude than on the N1 and N3 atoms.

Particularly interesting is the positive density on the bridging nitrogen atom N1 which refutes the spin polarization mechanism. However a spin polarization of the azido group does actually exist, besides the dominating spin delocalization phenomenon, as shown by the negative spin population carried by the central nitrogen atom of the N_3^- group.

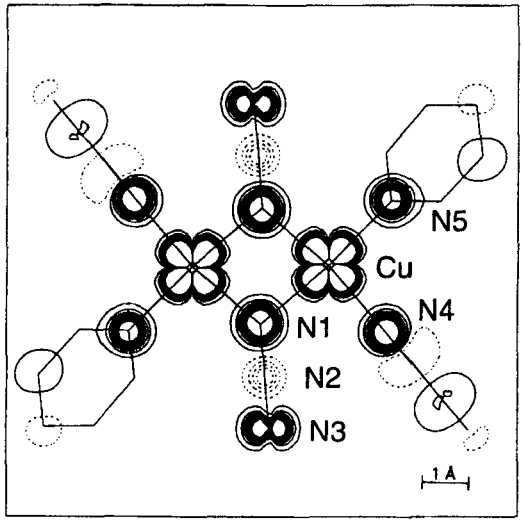

FIGURE 3 Induced spin density projection for $[Cu_2(t\text{-}Bupy)_4(N_3)_2](ClO_4)_2$ along a perpendicular to the (Cu-N1-Cu') plane at 1.6K under 4.6 Teslas. Same levels as in Fig. 1.

The spin distribution in the $[Cu_2(t\text{-}Bupy)_4(N_3)_2](ClO_4)_2$ compound presents some similarities with the spin distribution in the ferromagnetically coupled di-μ-hydroxo dicopper compound studied by p.n.d. by Figgis et

al.[4]. The spin density in $[Cu_2(OH)_2(bipy)_2(H_2O)(SO_4)].4H_2O$ is more localized on the copper ions ($0.847\mu_B$) than in the di-μ-1,1-azido compound. A positive spin population of $0.12\mu_B$ is observed on the bridging oxygen atoms as a result of the sum of the positive spin contributions transferred from both copper ions. Small spin populations of about $0.04\mu_B$ are found on the nitrogen atoms of the bipy ligands. The presence of negative regions of spin density in the vicinity of the bridging oxygen atoms indicates that spin polarization effects are also present.

FERROMAGNETIC CHAIN MN(II)NI(II) COMPOUND

The compound $MnNi(NO_2)_4(en)_2$ (with en = ethylenediamine) constitutes the first ferromagnetic chain bimetallic compound to be fully characterized, magnetically as well as structurally[12]. The chains present a zig-zag structure formed by alternating Mn(II) and Ni(II) ions bridged by a bidendate NO_2^- group. The structure can be described as a superimposition of ABAB layers perpendicular to the [001] direction: in the A layer the chains are parallel to [110] while in the B layer they are directed along the [-110] direction.

The two oxygen atoms of the bridging nitro group are linked to Manganese and the nitrogen atom is bonded to Nickel. The Nickel ion is located on an inversion center, in a nearly perfect octahedral environment. It is surrounded by four nitrogen atoms coming from the two ethylenediamine groups and by two NO_2^- bridging nitrogen atoms.

The Manganese ion resides on a two-fold symmetry axis and presents an unusual coordination sphere constituted by eight oxygens atoms, among which six are at a mean distance of 2.27 Å and two non bonding oxygen atoms at a slightly larger distance of 2.47 Å. These eight oxygen atoms originate from four NO_2^- groups surrounding the Mn(II) ion: two bridging nitro groups and two non bridging nitro groups which are bonded to Mn(II) by only one oxygen atom each. The intrachain Mn ... Ni distance is equal to 4.817Å.

Magnetic susceptibility measurements as function of temperature have given evidence for a weak intrachain ferromagnetic coupling J = 1.33 cm^{-1}. A long range antiferromagnetic ordering between the chains occurs at T_N = 2.35K. The behaviour of the magnetization versus magnetic field is characteristic of a metamagnetic compound with a threshold field of 1.2 KOe.

Nuclear scattering

The polarized neutron data treatment requires the knowledge of the nuclear structure factors at low temperature. Usually these structure factors are calculated from the precise nuclear structure, that means the atomic position parameters including those of the hydrogen atoms and the thermal parameters. The determination of the structure by X-ray diffraction at room temperature[12] did not allow to locate the hydrogen atoms, which is absolutely necessary because of their strong contribution to nuclear scattering. An unpolarized neutron diffraction experiment has therefore been performed at 20K, on the four-circle diffractometer 6T2 of the L.L.B., at the Orphée reactor, Saclay. The neutron beam was monochromated by a graphite monochromator providing a wavelength of 1.52Å.

A crystal of size (4.5 × 2.5 ×1) mm^3 with the long dimension along the $\vec{c}$ direction was set on the diffractometer and cooled down in a displex fridge. The cell parameters determined at 20K (a = 14.53(2)Å, b = 7.70(1)Å, c = 12.38(4)Å) indicate a decrease of the b and c values with respect to the room temperature parameters while the a value remains the same[12]. The integrated intensities of 773 unique reflections were measured. The structural refinement is in progress. In order to perform a preliminary analysis of the polarized neutron data, we have directly used the experimental nuclear structure factors. The observed nuclear structure factor $|F_N^{obs}|$ is given by the square root of the intensity after correction due to the Lorentz geometrical factor and absorption effects. The scale factor obtained by the structure refinement is then applied to $|F_N^{obs}|$ and the sign of the nuclear structure factor is deduced from the structure calculation.

Magnetic scattering

The polarized neutron measurements were performed on the polarized neutron diffractometer 5C1 of the L.L.B. A heusler polarizing monochromator provided a polarization rate of 0.92 for a wavelength of 0.84Å. A first data collection at 4K under an applied field of 2 Teslas was performed on a piece of the crystal (5 mm^3) which has been used for the structure experiment. The crystal was set on the two-axis diffractometer with the direction $\vec{c}$ vertical. A set of 82 unique hkl reflections was measured with $h_{max} = 11$, $k_{max} = 6$ and $l_{max} = 4$. A second data collection has been recently performed on a larger crystal of 15 mm^3 size with $\vec{b}$ vertical for hkl reflections with $h_{max} = 15$, $k_{max} = 3$ and $l_{max} = 9$. A second set of 82 unique reflections was obtained including 37 reflections common to the first set, leading to 164 reflections for the data treatment among which 127 were independent.

Because the Mn(II) and Ni(II) ions are located on special crystallographic positions, they do not contribute to magnetic scattering (assuming spherical magnetic form factors) for the hkl reflections following the extinction rules: (k and l odd, h even) and (k even and l odd, h even or odd). The measurement of the flipping ratios of these particular reflections allows to investigate directly the existence of magnetic moments delocalized on other atoms than Mn(II) or Ni(II).

Spin density map

The modelled spin density map is represented in Fig. 4., in projection along the perpendicular to the N1-Ni-N3 plane. As a first approximation, spherical atomic spin densities were refined and the model was restricted to the metal ions and their first neighbours. Only the low density levels are drawn in order to visualize the spin density delocalization. The spin density is positive over all the map including on the NO_2^- bridge. The spin transfer towards the bridging nitrogen atom appears to be weaker than towards each nitrogen atom of the ethylenediamine groups.

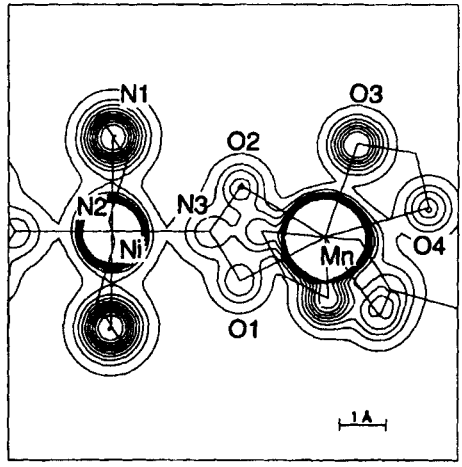

FIGURE 4 Induced spin density integrated along the perpendicular to the N1-Ni-N3 plane in the ferromagnetic chain compound $MnNi(NO_2)_4(en)_2$ at 4K under an applied field of 2 Teslas. Same levels as in Fig. 1.

The model parameters corresponding to this map are reported in Table I, as well as the reliability factor $R_w(F_M) = [(\Sigma_{hkl}\, w(\,|\,F_M^{obs}\,|\,-\,|\,F_M^{cal}\,|\,)^2\,/\,(\Sigma_{hkl}\, w\,|\,F_M^{obs}\,|\,^2)]^{1/2}$, with the weighting sheme $w = 1/\sigma^2$, and the goodness of fit $S = [(\Sigma_{hkl}\, w(\,|\,F_M^{obs}\,|\,-\,|\,F_M^{cal}\,|\,)^2)\,/\,(N_o - N_v)\,]^{1/2}$ with N_o = number of reflections and N_v = number of parameters. Twelve parameters were refined for 164 reflections used: the scale factor between the two sets of reflections (because of the slightly different values of the induced magnetization when the field is applied along the $\vec{b}$ axis or the $\vec{c}$ axis), the manganese and nickel radial exponents and nine monopole populations. The refined scale factor is equal to 1.133(17). The sum of the refined populations yields the value of 4.82 μ_B per MnNi unit for the induced magnetization, which was not determined by magnetic measurements. The spin populations given in Table I are normalized to 7 μ_B for each MnNi unit which corresponds to a system of local spins $S_{Mn^{2+}} = +\,5/2$ and $S_{Ni^{2+}} = +\,1$.

TABLE I Spin density Model Refinement: Reliability factors, Radial coefficients and Spin populations (normalized to 7 μ_B).

Reliability factors	
$R_w(F_M)$	0.082
S	2.0
Radial coefficients (au^{-1})	
ζ_{Mn}	7.36(8)
ζ_{Ni}	9.94(36)
Spin populations (μ_B)	
Mn	4.18(4)
Ni	1.68(4)
N1	0.19(3)
N2	0.10(4)
N3	0.04(3)
O1	0.04(3)
O2	0.04(3)
O3	0.10(1)
O4	0.04(3)

The spin populations associated to the atoms of the bridge are very small, 0.04(3)μ_B on each atom, and of the same order of magnitude than the error bar. Larger population values are found on atoms which do not belong to the bridge, up to 0.19(3)μ_B on N1. It is necessary to be cautious with such small populations which are more sensitive to the model than the main spin populations on Mn(II) and Ni(II). However the occurence of spin delocalization is demonstrated by the observation of non-zero magnetic contributions on the reflections to which the Mn(II) and Ni(II) ions do not contribute magnetically. The Table II displays the experimental flipping ratios and magnetic structure factors (with $F_M > \sigma$) determined for such reflections, together with the values calculated from the spin density refinement.

TABLE II Flipping ratios, Observed and Calculated Magnetic structure factors due to Spin Delocalization only.

Flipping ratios and Magnetic structure factors (in μ_B)			
hkl	R_{exp}	F_M^{obs}	F_M^{cal}
2 1 1	1.038(12)	0.25(7)	0.10
4 1 1	1.043(19)	-0.19(8)	-0.15
2 2 1	1.030(13)	-0.48(18)	-0.17
4 2 1	0.947(38)	-0.36(25)	-0.36
5 2 1	0.971(16)	-0.36(17)	-0.36
1 2 3	0.948(28)	0.22(16)	0.24

The delocalization from the nickel ion towards the bridging N3 atom of the nitro group is clearly weaker than towards the N1 ($0.19(3)\mu_B$) and N2 ($0.10(4)\mu_B$) atoms of the ethylenediamine groups. Similarly the spin transfer from Mn^{2+} is smaller on both oxygen atoms O1 and O2 of the bridge than on the O3 atom of the non-bridging NO_2^- groups. The weak spin population on the oxygen atom O4 may be explained by the larger distance Mn-O4 distance.

The sum of the metal ion population and its first neighbours is equal to $2.3(1)\mu_B$ for the nickel and six nitrogen atoms on one side and to $4.7(1)\mu_B$ for the manganese and eight oxygen atoms on the other side. The quantity of spin transferred from the Mn^{2+} to its neighbours only amounts to 10 per cent of the moment associated to the manganese region while the spin delocalization from Ni^{2+} represents 29 per cent of the total moment on the nickel site. The Ni - N mean distance (2.16Å) is shorter than the Mn-O mean bond length (2.27 Å) in the Mn(II)Ni(II) compound.

Discussion

A different bridging geometry of the NO_2^- group may be found in the famous NENP compound[21], which forms -Ni-NO_2-Ni- chains with antiferromagnetically coupled nickel spins S=1. In this case the two metal ions are Ni^{2+} ions and the nitro group does not bridge in a bidendate fashion. The

nitrogen atom is linked to one Ni^{2+} ion and only one oxygen atom is linked to the other Ni^{2+} ion. The AF coupling along the chain was attributed to the efficient overlap between the nickel magnetic orbitals via the Ni-N and Ni-O spin delocalization on the NO_2^- bridge.

The study of covalent bonding in $Ni(ND_3)_4(NO_2)_2$[22] provides interesting informations about the spin transfer from the Ni^{2+} ion towards NO_2^-. In this compound the nickel ion lies in an octahedral environment formed by four ND_3 group and two NO_2^- groups. The spin is mainly located in the d_{xy} and d_{z^2} orbitals of the nickel ion. The spin population on the ligands represents 27 per cent of the total spin ($2\mu_B$). A positive spin density ($0.10(2)\mu_B$) is delocalized on the nitrogen atom of the nitro group. No significant population was found on the oxygen atoms of the NO_2^- group. The spin transfer towards the nitrogen of the ammonia molecule is slightly smaller ($0.08(1)\mu_B$). The spin density map shows that the Ni-NO_2 and Ni-ND_3 bondings are σ antibonding. The antibonding nature is reflected by the presence of negative spin density in the Ni- nitro bond and in the Ni- ammonia bond.

Unlike this compound, the Mn(II)Ni(II) compound apparently presents a negligible spin transfer from the Ni^{2+} ion towards the nitrogen atom of the NO_2^- bridging group. This can be interpreted by a reduction of the positive spin actually delocalized on this nitrogen atom by a negative contribution due to the presence of the Mn^{2+} ion. In a reciprocical way, the spin delocalization from the Mn^{2+} ion towards the oxygen atoms of the nitro bridge would be almost compensated by a negative contribution arising from Ni^{2+}. Spin polarization effects can be responsible for such negative contributions and the spin distribution on the bridge in Mn(II)Ni(II) would result from a balance between the spin delocalization and spin polarization mechanisms.

CONCLUSION

P.n.d. investigations of the spin density in bimetallic compounds provide most valuable informations about the respective roles of spin delocalization and spin

polarization in the setting up of AF or ferromagnetic intramolecular interactions. The spin density maps in AF coupled bimetallic compounds vizualize the spin delocalization onto the bridge which ensures a strong overlap of the magnetic orbitals centered on each magnetic center. The p.n.d. study of a ferromagnetically coupled di-μ-1,1-azido Cu^{2+} binuclear compound has allowed to refute the spin polarization mechanism and to show that the spin distribution is dominated by the spin delocalization phenomenon on which is superimposed a spin polarization of the azido bridge. Finally the spin distribution along the ferromagnetic chain in the NO_2-bridged Mn(II)Ni(II) compound could result from an interference between the spin delocalization and spin polarization effects.

Acknowledgments

The author express her deepest gratitude to Professor O. Kahn, from the Institut de Chimie de la Matière Condensée de Bordeaux, who initiated the works presented here and thanks him for many rich discussions. The author thanks C. Mathonière and T. Rajendiran (I.C.M.C.B.) for the Mn(II)Ni(II) single crystal elaboration and A. Gukasov (L.L.B.) for his help in the low temperature experiments for the Mn(II)Ni(II) structural study.

References

[1] J.B. Forsyth, *Atomic Energy Review,* **172,** 345 (1979).
[2] P.J. Brown, A. Capiomont, B. Gillon and J. Schweizer, *J. Magn. Magn. Mat.,* **14,** 289 (1979).
[3] G.A. Williams, B.N. Figgis and R. Mason, *J. Chem. Soc. Dalton Trans.,* **734** (1981).
[4] B.N. Figgis, R. Mason, A.R.P. Smith, J.N. Varghese and G.A. Williams, *J. Chem. Soc. Dalton Trans.,* 703 (1983).
[5] B. Gillon, C. Cavata, P. Schweiss, Y. Journaux, O. Kahn and D. Schneider, *J. Am. Chem. Soc.,* **111,** 7124 (1989).
[6] O. Kahn, in *Molecular Magnetism* (New York:VCH Publishers, Inc., 1993), p. 305, 149, 163.
[7] V. Baron, B. Gillon, O. Plantevin, A. Cousson, C. Mathonière, O. Kahn, A. Grand, L. Öhrström and B. Delley, *J. Am. Chem. Soc.,* **118,** 11822 (1996).
[8] V. Baron, B. Gillon, A. Cousson, C. Mathonière, O. Kahn, A. Grand, L. Öhrström, B. Delley, M. Bonnet and J.X. Boucherle, *J. Am. Chem. Soc.,* **119,** 3500 (1997).
[9] L.K. Thomson, S.S. Tandon and M.E. Manuel, *Inorg. Chem.,* **34,**2356 (1995).
[10] M.A. Aebersold, O. Kahn, P. Bergerat, O. Plantevin, L. Pardi, B. Gillon, I. von Seggern, F. Tuczek, L. Öhrström, A. Grand and E. Lelièvre-Berna, *J. Am. Chem. Soc.,* **120,** 5238 (1998).
[11] S. Sikorav, I. Bkouche-Waksman and O. Kahn, *Inorg. Chem.,* **23,** 490 (1984).
[12] O. Kahn, E. Bakalbassis, C. Mathonière, M. Hagiwara, K. Katsumata and L. Ouahab, *Inorg. Chem.,* **36,** 1530 (1997).

[13] E. Ressouche, A. Zheludev, J.X. Boucherle, B. Gillon, P. Rey and J. Schweizer, *Mol. Cryst. Liq. Cryst.*, **233,** 13 (1993).
[14] C. Kittel, in *Introduction to Solid State Physics, 6th ed.* (New York, Wiley J & Sons, 1986), p. 405.
[15] G.L. Squires, in *Introduction to the theory of thermal neutron scattering*(Cambridge: University Press, 1978), p. 139.
[16] R.J. Papoular and B. Gillon, *Europhys. Lett.*, **13,** 429 (1990).
[17] V. Baron, B. Gillon, C. Mathonière, O. Kahn, M. Bonnet and J.X. Boucherle, *Mol. Cryst. Liq. Cryst.*, **233,** 247 (1993).
[18] E. Ressouche, thesis, Université J. Fourier, Grenoble (1991).
[19] C. Mathonière, O. Kahn, J.C. Daran, H. Hilbig and F.H. Köhler, *Inorg. Chem.*, **32,** 4057 (1993).
[20] O. Kahn, C. Mathonière, B. Srinavasan, B. Gillon, V. Baron, A. Grand, L. Öhrström and S. Ramashesha, *New J. Chem.*, **21,** 1037 (1997).
[21] A. Meyer, A. Gleizes, J.J. Girerd, M. Verdaguer and O. Kahn, *Inorg. Chem.*, **21,** 1729 (1982).
[22] B.N. Figgis, P.A. Reynolds and R. Mason, *J. Am. Chem. Soc.*, **105,**440 (1983).